ResearchGate

See discussions, stats, and author profiles for this publication at: https://www.researchgate.net/publication/231184445

Equations for calculation of chromatographic figures of merit for ideal and skewed peaks

ARTICLE *in* ANALYTICAL CHEMISTRY · APRIL 1983

Impact Factor: 5.64 · DOI: 10.1021/ac00255a033

CITATIONS
368

READS
22

2 AUTHORS, INCLUDING:

Joe P. Foley
Drexel University
108 PUBLICATIONS **3,261** CITATIONS

SEE PROFILE

Available from: Joe P. Foley
Retrieved on: 30 January 2016

(3) Amatels, P. G.; Taylor, L. T., submitted to *J. Chromatogr.*
(4) Schabron, J. F.; Hurtubise, R. J.; Silver, H. F. *Anal. Chem.* **1979**, *51*, 1426.
(5) Brown, R. S.; Hellgeth, J. W.; Taylor, L. T. Presented at the 8th FACSS Meeting, Philadelphia, PA, Sept 1981.
(6) Johnson, C. C.; Taylor, L. T. *Anal. Chem.*, in press.
(7) Brown, R. S.; Hausler, D. W.; Taylor, L. T.; Carter, R. C. *Anal. Chem.* **1981**, *53*, 197.
(8) Rudnick, L. R.; Whitehurst, D. D. *ACS Symp. Ser.* **1981**, *No. 169*, 153.

RECEIVED for review September 8, 1982. Accepted December 22, 1982. The financial assistance provided by Department of Energy Grant DE-FG22-81PC40799 and the Commonwealth of Virginia is gratefully appreciated.

Equations for Calculation of Chromatographic Figures of Merit for Ideal and Skewed Peaks

Joe P. Foley and John G. Dorsey*

Department of Chemistry, University of Florida, Gainesville, Florida 32611

By use of the exponentially modified Gaussian (EMG) as the skewed peak model, empirical equations based solely on the graphically measurable retention time, t_R, peak width at 10% peak height, $W_{0.1}$, and the empirical asymmetry factor, B/A, have been developed for the accurate and precise calculation of parameters (termed chromatographic figures of merit (CFOMs)) characterizing both ideal (Gaussian) and skewed chromatographic peaks. These CFOMs include: the number of theoretical plates (observed efficiency), N_{SYS}; the maximum efficiency attainable if all asymmetry is eliminated, N_{MAX}; the EMG peak parameters, t_G, σ_G, and τ; the first through fourth statistical moments; the peak skew and peak excess, γ_S and γ_E; and two new CFOMs—the relative system efficiency, RSE, and the relative plate loss, RPL. Equations for the number of theoretical plates and the second central moment (variance) are accurate to within ±1.5% for $1.00 \leq B/A \leq 2.76$. Width and B/A measurements at 10% peak height are recommended.

In recent years there has been considerable interest in the characterization of experimental chromatographic peaks. Presented in Table I are the names, symbols, and general expressions that have evolved for the parameters used in chromatographic peak characterization. It is proposed that these parameters be referred to collectively as chromatographic figures of merit (CFOMs).

These CFOMs have been estimated either by hand (manual) calculation using graphical measurements made directly from the chromatogram or by a computer following data acquisition. Both methods have advantages and disadvantages.

Manual methods were used exclusively at first and are employed quite extensively today. For arbitrary peak shapes, they are accurate for only five CFOMs: t_R, B/A, h_P, W_b, and W_α. If a Gaussian peak shape is assumed, however, then $M_1 = t_R$, and $\bar{M}_2$ is only a function of W_b, W_α, or M_0, and N may be subsequently calculated. Except for higher *even* central moments, the remaining CFOMs are zero for Gaussian peaks.

For real chromatographic peaks, it is almost always a mistake to assume a Gaussian peak shape. Experimentally these ideal symmetric peaks are rarely, if ever, observed due to various intracolumn and extracolumn sources of asymmetry (*1–13*). Pauls and Rogers, for example, have shown that the variance of an asymmetric peak can be underestimated by more than 50% (*9*) if the Gaussian width at half-height equation is used. Kirkland et al. have demonstrated that the plate count can be overestimated by as much or more than 100% if any of the three most common Gaussian-based equations are employed (*10*).

Computer estimation methods are more accurate than common manual methods for a given CFOM but are not available to every chromatographer. The general approach taken has been one of peak statistical moment analysis (*3, 7, 10, 11, 14, 15*). Via relatively simple algorithms all the CFOMs may be determined quite accurately, though the precision of the second and higher central moments is seriously affected by base line noise (*16*).

The failure of the Gaussian function as a peak shape model for real chromatographic peaks led to the search for a more accurate model and the eventual acceptance of the exponentially modified Gaussian (EMG). The development, characterization, and theoretical and experimental justification of this model has been thoroughly reviewed (*9, 11, 14, 17*).

Application of the EMG peak model yields a new set of CFOMs given in Table II; this set consists of fundamental and derived EMG parameters, the latter containing explicit expressions for the first through fourth statistical moments defined previously in Table I. Included among the new CFOMs are the following: the retention time, t_G, and standard deviation, σ_G, of the associated parent Gaussian peak from which the skewed EMG peak is derived; the exponential modifier, τ; the fundamental ratio, τ/σ_G, which characterizes peak asymmetry; the observed efficiency (number of theoretical plates) of a given (asymmetric) chromatographic system, N_{SYS}; the maximum efficiency a given system could achieve, N_{MAX}, if all sources of asymmetry were eliminated; and finally, two CFOMs proposed originally in this work which demonstrate dramatically how peak asymmetry drastically reduces chromatographic efficiency—the relative system efficiency, RSE, and the relative plate loss, RPL.

Adoption of the EMG peak-shape model has improved the estimation of the CFOMs. A new algorithm for the computer-based peak moment analysis has been derived (*17*) and tested (*11*) which is less sensitive to base line noise and the uncertainty of peak start/stop assignments. More recently, Barber and Carr described a manual method for CFOM quantitation which requires the graphically measurable retention time t_R, peak width W_α, empirical asymmetry factor B/A, and successive interpolations from three large-scale, universal calibration curves (*18, 19*).

The purpose of the present work was to develop accurate equations for CFOM calculation dependent solely on t_R, $W_{0.1}$, and B/A. The need for computerized data acquisition is thus circumvented, and, in addition, this method is faster and

0003-2700/83/0355-0730$01.50/0 © 1983 American Chemical Society

Table I

Common Chromatographic Figures of Merit

parameter	symbol	general expression
theoretical plates	N	(retention time)^2/variance
retention time	t_R	peak maximum
	M_1	peak centroid
	t_m	peak median
empirical asymmetry factor	B/A	see Figure 1
peak height	h_p	
peak width at specified height	W_α	α denotes peak height fraction
peak width at base	W_b	tangents drawn from inflection points
peak shape function	$h(t)$	

Statistical Moments and Related Quantities

zeroth (peak area)	M_0	$\int_{-\infty}^{\infty} h(t)\,dt$
first (peak centroid)	M_1	$\int_{-\infty}^{\infty} th(t)\,dt/M_0$
2nd central moment (variance)	$\bar{M}_2$	$\int_{-\infty}^{\infty} (t-M_1)^2 h(t)\,dt/M_0$
nth central moment	$\bar{M}_n$	$\int_{-\infty}^{\infty} (t-M_1)^n h(t)\,dt/M_0$
peak skew	γ_S	$\bar{M}_3/\bar{M}_2^{3/2}$
peak excess	γ_E	$\bar{M}_4/\bar{M}_2^2 - 3$

Table II. Chromatographic Figures of Merit Based on Exponentially Modified Gaussian Model

Fundamental

$t_G,\ \sigma_G,\ \tau,\ \tau/\sigma_G$

Derived

$$N_{SYS} = t_R^2/(\sigma_G^2 + \tau^2)$$

$$N_{MAX} = (t_G/\sigma_G)^2$$

$$RSE = \frac{N_{SYS}}{N_{MAX}}\left(\frac{t_G}{t_R}\right)^2 = \frac{\sigma_G^2}{\bar{M}_2}$$

$$RPL = \left(\frac{N_{MAX} - N_{SYS}}{N_{MAX}}\right)\left(\frac{t_G}{t_R}\right)^2 = 1 - RSE = \frac{\tau^2}{\bar{M}_2}$$

$$M_1 = t_G + \tau$$

$$\bar{M}_2 = \sigma_G^2 + \tau^2$$

$$\bar{M}_3 = 2\tau^3$$

$$\bar{M}_4 = 3\sigma_G^4 + 6\sigma_G^2\tau^2 + 9\tau^4$$

$$\gamma_S = \bar{M}_3/\bar{M}_2^{3/2}$$

$$\gamma_E = \bar{M}_4/\bar{M}_2^2 - 3$$

somewhat more precise than the other accurate manual method since no graphical interpolation is required.

DERIVATIONS

If a Gaussian peak shape equation G is used to approximate the true value T of a CFOM for an asymmetric peak, the relative error RE which results is defined as

$$RE = (G - T)/T \tag{1}$$

which can be rearranged to give

$$T = G/(RE + 1) \tag{2}$$

Thus, the true value T and the Gaussian approximation G for the CFOM are related by the correction term (RE + 1) in the denominator of eq 2.

Kirkland et al. have shown that

$$RE = f(\tau/\sigma_G) \tag{3}$$

for the three popular Gaussian-based methods for determining plate counts of a system (*10*). Equation 3 should hold, in fact, for any CFOM for which a Gaussian approximation exists except t_G. Since Barber and Carr have shown (*18*) that

$$\tau/\sigma_G = f(B/A) \tag{4}$$

successive substitution of eq 3 and 4 into eq 2 yields

$$T = G/[f(B/A) + 1] \tag{5}$$

Although the exact form of $f(B/A)$ is unknown, a least-squares curve fitting of an RE vs. B/A plot can suffice as an approximation.

The above approach was used for calculation of N_{SYS}, σ_G, and $\bar{M}_2$. Following this, τ was calculated (see sixth equation, Table II) by

$$\tau = \sqrt{\bar{M}_2 - \sigma_G^2} \tag{6}$$

For determination of t_G, the universal relationship

$$(t_R - t_G)/\sigma_G = f(\tau/\sigma_G) \tag{7}$$

previously described (*18*) was rearranged and combined with eq 4 to give

$$t_G = t_R - \sigma_G f(B/A) \tag{8}$$

where $f(B/A)$ was approximated by a least-squares fit of $(t_R - t_G)/\sigma_G$ vs. B/A.

Since t_R, B/A, and $W_{0.1}$ are graphically measurable, all the remaining CFOMs can be calculated once the fundamental parameters σ_G, τ, and t_G have been determined.

EXPERIMENTAL SECTION

Apparatus. An Apple II Plus 48K microcomputer was programmed in BASIC for EMG peak generation. A curve-fitting program available from Interactive Microware with linear, geometric, exponential, and polynomial capabilities was used for the unweighted least-squares fitting of various data sets.

EMG Peak Generation. An exponentially modified Gaussian peak can be given (*14*) by

$$f(t) = \frac{A^*\sigma_G}{\tau\sqrt{2}} \exp\left[\left(\frac{\sigma_G}{\tau}\right)^2 \frac{1}{2} - \frac{(t - t_G)}{\tau}\right] \int_{-\infty}^{Z} \exp[-x^2]\,dx \tag{9}$$

where

$$Z = [(t - t_G)/\sigma_G - \sigma_G/\tau]/\sqrt{2} \tag{10}$$

Via change of variable the integral in eq 9 is transformed to

$$\sqrt{\pi} \int_{-\infty}^{Z\,2^{1/2}} \frac{\exp[-y^2/2]}{\sqrt{2\pi}}\,dy$$

and the EMG function can now be written as

$$f(t) = \frac{A^*\sigma_G}{\tau}\sqrt{\frac{\pi}{2}} \exp\left[\left(\frac{\sigma_G}{\tau}\right)^2 \frac{1}{2} - \frac{(t - t_G)}{\tau}\right] \int_{-\infty}^{Z\,2^{1/2}} \frac{\exp[-y^2/2]\,dy}{\sqrt{2\pi}} \tag{11}$$

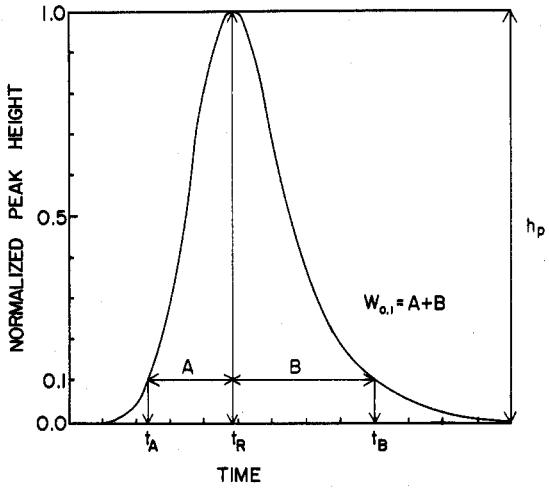

Figure 1. Measurement of retention time, t_R; peak width, $W_{0.1}$; and asymmetry factor, B/A, at peak height fraction $\alpha = 0.1$ required for equations in Table III. Analogous measurements at $\alpha = 0.3$, 0.5 are needed for equations in Tables IV and V, respectively. Except for A, B, and B/A at $\alpha = 0.1$, all width-related measurements are subscripted with the value of α to prevent ambiguity.

where A^* is the peak amplitude, τ is the exponential modifier, σ_G and t_G are the standard deviation and retention time, respectively, of the parent Gaussian, and y is a dummy variable of integration. For fixed A^*, τ, σ_G, and t_G, $f(t)$ is defined over an infinite continuum of time. Calculation of $f(t)$ was facilitated by use of a polynomial approximation $P(Z2^{1/2}, Z2^{1/2} \geq 0)$ in error by less than 7.5×10^{-8} for the integral in eq 11 (*20*). When $Z2^{1/2} < 0$, the integral may be calculated from $1 - P(-Z2^{1/2})$.

Procedure. Except as otherwise noted, values of $A^* = 1$, $t_G = 100$, and $\sigma_G = 5$ were used in eq 11 for EMG peak generation. The τ/σ_G ratio was varied from 0.1 to 3 in 0.05 increments producing data equivalent to 59 peaks. The times for t_R, t_A, and t_B (see Figure 1) at $\alpha = 0.1$, 0.3, and 0.5 for each of the 59 peaks were determined to within 0.001, using a simple search algorithm; corresponding values of W and B/A were then computed. When values for $W_{0.1}$, B/A, and $(t_R - t_G)/\sigma_G$ for the 59 peaks were compared with analogous data obtained elsewhere (*19*), the maximum relative average deviations observed were 25 ppm, 405 ppm, and 668 ppm, respectively.

Textfiles of RE (N_{SYS}, $\bar{M}_2$, σ_G) vs. $(B/A)_{0.1,0.3,0.5}$, $(t_R - t_G)/\sigma_G$ vs. $(B/A)_{0.1,0.3,0.5}$, and RSE vs. B/A were made for $0.1 \leq \tau/\sigma_G \leq 3$. The Gaussian relations $\sigma_G = W_{0.1}/4.291932$ and $\bar{M}_2 = (W_{0.1}/4.291932)^2$ were used in the calculation of the Gaussian approximations for N_{SYS}, σ_G, and $\bar{M}_2$ at $\alpha = 0.1$. Similar equations were used for $\bar{M}_2$ and σ_G at $\alpha = 0.3$, 0.5. The true values of N_{SYS}, σ_G, $\bar{M}_2$, and RSE were computed from the known values of τ, σ_G, t_G, and t_R for a given peak. Although the least-squares fittings of the various B/A textfiles were initially judged by visual inspection and the coefficient of determination, their final evaluation was based on the accuracy and simplicity of the resulting CFOM equations.

The relationship between several quantities [e.g., RE(N), $(B/A)_\alpha$, W_α] and τ/σ_G has been shown previously (*10*, *18*) to be nonlinear for $0 < \tau/\sigma_G < 0.5$ and nearly linear for $0.5 \leq \tau/\sigma_G \leq 3$. Because similar relationships were observed in some of the textfiles above, least-squares fitting was limited to about the same τ/σ_G range 0.5–3 ($1.09 \leq B/A \leq 2.76$) except for the RSE vs. B/A textfile where the complete set of values was used in the regression analysis.

For ease of use, the CFOM equations were simplified first by algebraic factorization and cancellation and then by successive rounding of numerical coefficients. The occasional nearness of the decimal coefficients to whole numbers was exploited. For example, if $f(B/A) = 1.02(B/A) + 0.69$, then for $1.09 \leq B/A \leq 2.76$ the much simpler function $f(B/A) = B/A + 0.72$ is approximately the same (exactly if $B/A = 1.5$) and the accuracy of this function is not significantly affected.

All CFOM equations were simplified as much as possible—any more rounding of the coefficients will result in appreciably greater error.

The accuracy of the CFOM equations was evaluated in terms of four parameters, listed in decreasing order of importance: the percent relative error limits (%RELs) which represent the maximum possible error of the CFOM equations within the specified B/A range; the mean percent relative error or bias $\%\overline{RE} \equiv \sum \%RE/n$; the average magnitude of the percent relative error $\sum|\%RE|/n$; and the standard deviation of the percent relative error. The last three parameters are not specified for each CFOM in this report but may be obtained upon request.

The precision of the empirical, EMG-based CFOM equations and three Gaussian CFOM equations was calculated via error propagation theory (*21*) and is reported as percent relative standard deviation (%RSD). The required precision estimates of t_R, W_α, and $(B/A)_\alpha$ [the graphically measurable quantities] were obtained by using data from a previous study (*19*).

RESULTS AND DISCUSSION

Listed in Table III are the empirical CFOM equations based on t_R, $W_{0.1}$, and B/A measurements (see Figure 1) which we recommend.

Accuracy. By use of eq 1 in Table III, the true efficiency of a chromatographic system, N_{SYS}, *may be estimated to within ±1.5% for both Gaussian and exponentially tailed peaks* within the asymmetry range $1.00 \leq B/A \leq 2.76$. Equations for $\bar{M}_2$, t_G, and M_1 also achieve this accuracy and range.

All CFOMS except RPL, $\bar{M}_3$, γ_S, and γ_E can be estimated to within ±5% for $1.09 \leq B/A \leq 2.76$, the asymmetry range over which most of the curve fitting was performed.

All CFOM equations are accurate to within ±5% for $1.19 \leq B/A \leq 2.76$, and 18 out of 21 are accurate to within ±2%.

Except for eq 11b, 13b, and 14b which had biases of +0.976%, +0.820%, and +1.111%, respectively, the bias for every equation given in Tables III, IV, and V was less than ±0.6%.

Precision Summary. For the equations in Table III, the estimated relative standard deviation (RSD) limits obtained via propagation of error theory for N_{SYS}, $\bar{M}_2$, σ_G, N_{MAX}, and RSE were all less than or equal to ±4.5%. RSD limits for t_G and M_1 were ±0.2%.

The precision of the EMG equations in Table III, the width-based Gaussian equations, and the calibration curve method of Barber and Carr (*18*) is compared for N_{SYS}, $\bar{M}_2$, and σ_G in Table VI. The results shown for the Gaussian equations are valid for 50%, 30%, and 10% width measurements because $RSD(W_{0.5}) = RSD(W_{0.3}) = RSD(W_{0.1})$. The slightly greater imprecision observed for the EMG equations is due to uncertainty in the B/A measurement not required for the Gaussian equations. The somewhat larger %RSDs for the method of Barber and Carr are probably due to interpolation uncertainties (from the calibration curves) unique to this method.

The precision of the remaining CFOMs in Table III was found to be highly dependent on the peak shape. Rather than reporting RSD limits, the RSD for several CFOMs or groups of CFOMs has been plotted vs. B/A in Figure 2.

Other Equations. Listed in Table IV and V are smaller sets of CFOM equations developed *only* for use in determining if a real chromatographic peak is well-modeled by an EMG peak and should *not* be used to routinely calculate any CFOM (including N_{SYS}) since they are usually less accurate, less precise, and more complex than the analogous equations in Table III. However, the accuracy and precision for $\bar{M}_2$, σ_G, t_G, and τ at $\alpha = 0.3$ and 0.5 is still sufficient to permit peak modeling decisions to be made.

Detailed Discussion of Precision. Shown in Table VII are the precision data for t_R, W_α, and $(B/A)_\alpha$ used in this study. The RSD results were obtained by converting previously reported raw precision data (*19*) to the form appropriate for error propagation analysis for the conditions specified in

Table III. Recommended Equations for Chromatographic Figures of Merit[a]

no.	equation	asymmetry range (B/A)	% rel error limits	% RSD limits
1	$N_{SYS} = \frac{41.7\,(t_R/W_{0.1})^2}{B/A + 1.25}$	1.00-2.76 2.77-4.00	−1.5, +1 −10, −1.5	±2.5
2a	$\overline{M}_2 = \frac{W_{0.1}^2}{1.764(B/A)^2 - 11.15\,(B/A) + 28}$	1.00-2.76	−1.5, +0.5	±2.2
2b	$\overline{M}_2 = t_R^2/N_{SYS}$	1.00-2.76	−1, +1.5	±2.4
3	$\sigma_G = \frac{W_{0.1}}{3.27\,(B/A) + 1.2}$	1.09-2.76	−1, +0.5[b]	±2.0
4a	$\tau = \sqrt{\overline{M}_2\ (\text{eq 2a}) - \sigma_G^2}$	1.09-2.76	−1, +3.5[c]	*f*
4b	$\tau = \sqrt{\overline{M}_2\ (\text{eq 2b}) - \sigma_G^2}$	1.09-2.76	−0.5, +5[c]	*f*
5a	$\frac{\tau}{\sigma_G} = \frac{\tau\ (\text{eq 4a})}{\sigma_G}$	1.09-2.76	−1, +4.5[c]	*f*
5b	$\frac{\tau}{\sigma_G} = \frac{\tau\ (\text{eq 4b})}{\sigma_G}$	1.09-2.76	−0.5, +6[c]	*f*
6	$t_G = t_R - \sigma_G[-0.193\,(B/A)^2 + 1.162\,(B/A) - 0.545]$	1.00-2.76	±0.5[d]	±0.2
7	$N_{MAX} = \left(\frac{t_G}{\sigma_G}\right)^2$	1.09-2.76	−0.5, +1[d]	±2.0
8	$RSE = 0.99\,(B/A)^{-2.24}$	1.00-2.76	±2	±4.5
9	$RPL = 1 - RSE$	1.09-2.76	−6, +1.5[c]	*f*
10	$\overline{M}_1 = t_G + \tau$ (eq 4a or eq 4b)	1.00-2.76	±1[d]	±0.2
11a	$\overline{M}_3 = 2\tau^3_{\text{eq 4a}}$	1.09-2.76	−2.5, +10.5[c]	*f*
11b	$\overline{M}_3 = 2\tau^3_{\text{eq 4b}}$	1.09-2.76	−1.5, +16[e]	*f*
12a	$\overline{M}_4 = 3\sigma_G^4 + 6\sigma_G^2\tau_{4a}^2 + 9\tau_{4a}^4$	1.09-2.76	−3, +1.5	*f*
12b	$\overline{M}_4 = 3\sigma_G^4 + 6\sigma_G^2\tau_{4b}^2 + 9\tau_{4b}^4$	1.09-2.76	−2, +3.5	*f*
13a	$\gamma_S = \frac{\overline{M}_3\ (\text{eq 11a})}{\overline{M}_2^{3/2}\ (\text{eq 2a})}$	1.09-2.76	−1, +10[c]	*f*
13b	$\gamma_S = \frac{\overline{M}_3\ (\text{eq 11b})}{\overline{M}_2^{3/2}\ (\text{eq 2b})}$	1.09-2.76	−0.5, +14.5[e]	*f*
14a	$\gamma_E = \frac{\overline{M}_4\ (\text{eq 12a})}{\overline{M}_2^2\ (\text{eq 2a})} - 3$	1.09-2.76	−1.5, +14[c]	*f*
14b	$\gamma_E = \frac{\overline{M}_4\ (\text{eq 12b})}{\overline{M}_2^2\ (\text{eq 2b})} - 3$	1.09-2.76	−0.5, +19.5[e]	*f*

[a] Based on t_R, $W_{0.1}$, and B/A measurements depicted in Figure 1. B/A measurements should be made to two decimal places. Numerical coefficients should not be rounded further (see Procedure). [b] Error limits are −4%, −1% for $1.00 \leq B/A \leq 1.09$. [c] Error limits are ±2% or less for $1.19 \leq B/A \leq 2.76$. [d] Error limits reported for $t_G/\sigma_G = 20$. For $t_G/\sigma_G > 20$, the error limits will be smaller than those reported. [e] Error limits are between ±2% and ±5% for $1.19 \leq B/A \leq 2.76$. [f] Precision of this CFOM is a function of peak shape. See plot of %RSD vs. B/A in Figure 2.

Table IV. Equations for Use Only in Peak Modeling[a]

equation	% rel error limits[b]	%RSD limits[b]
$N_{SYS} = \frac{6.88\,(t_R/W_{0.3})^2}{(B/A)_{0.3} - 0.3}$	±2	±4.0
$\overline{M}_2,a = \frac{W_{0.3}^2}{-3.85\,(B/A)_{0.3}^3 + 23\,(B/A)_{0.3}^2 - 47.9\,(B/A)_{0.3} + 38.7}$	−0.5, +1	±4.0
$\overline{M}_2,b = t_R^2/N_{SYS}$	±2	±4.1
$\sigma_G = \frac{W_{0.3}}{2.8\,(B/A)_{0.3} + 0.48}$	−2, +1	±2.5
$\tau, a = \sqrt{\overline{M}_2, a - \sigma_G^2}$	−0.5, 6[c]	*d*
$\tau, b = \sqrt{\overline{M}_2, b - \sigma_G^2}$	−1.5, +9.5[e]	*d*
$t_G = t_R - \sigma_G(0.6\,(B/A)_{0.3}^2 + 2.58\,(B/A)_{0.3} - 1.58)$	±0.5[f]	±0.2

[a] Based on t_R, $W_{0.3}$, and $(B/A)_{0.3}$ measurements. $(B/A)_{0.3}$ measurements should be made to two decimal places. Numerical coefficients should not be rounded further (see Procedure). [b] Valid for $1.09 \leq (B/A)_{0.1} \leq 2.76$. [c] Error limits are −0.5%, +2% for $1.19 \leq (B/A)_{0.1} \leq 2.76$. [d] Precision ranges from ±13.9% at $(B/A)_{0.1} = 1.09$ to ±2.0% at $(B/A)_{0.1} = 2.76$ in a manner similar to the τ, τ/σ_G curve shown in Figure 2. [e] Error limits are −1.5%, +4% for $1.19 \leq (B/A)_{0.1} \leq 2.76$. [f] Error limits reported for $t_G/\sigma_G = 20$ for $t_G/\sigma_G > 20$, the error limits will be smaller than those reported.

Table VII. Data excluded in the previous study for $(B/A - 1)_\alpha$ was also excluded in this analysis. The RSDs of t_R, W_α, and $(B/A)_\alpha$ for individual peak shapes (at a given peak height fraction) were averaged as done previously, thereby implicitly

Table V. Equations for Use Only in Peak Modeling[a]

equation	% rel error limits[b]	% RSD limits[b]
$N_{SYS} = \frac{1.83(t_R/W_{0.5})^2}{(B/A)_{0.5} - 0.7}$	±2	±9.4
$\bar{M}_2,a = \frac{W_{0.5}^2}{-8.28\,(B/A)_{0.5}^3 + 41.8\,(B/A)_{0.5}^2 - 72.3\,(B/A) + 44.6}$	−1, +2	±7.7
$\bar{M}_2,b = t_R^2/N_{SYS}$	±2	±9.4
$\sigma_G = \frac{W_{0.5}}{2.5\,(B/A)_{0.5}}$	±2	±3.2
$\tau,a = \sqrt{\bar{M}_2,a - \sigma_G^2}$	−1, +5.5[c]	*d*
$\tau,b = \sqrt{\bar{M}_2,b - \sigma_G^2}$	−1, +2.5	*d*
$t_G = t_R - \sigma_G(-1.46\,(B/A)_{0.5}^2 + 5\,(B/A)_{0.5} - 3.14)$	±0.5[e]	±0.2

[a] Based on t_R, $W_{0.5}$, and $(B/A)_{0.5}$ measurements. $(B/A)_{0.5}$ measurements should be made to two decimal places. Numerical coefficients should not be rounded further (see Procedure). [b] Valid for $1.09 \leq (B/A)_{0.1} \leq 2.76$. [c] Error limits are −1%, +2% for $1.19 \leq (B/A)_{0.1} \leq 2.76$. [d] Precision ranges from ±24.5% at $(B/A)_{0.1} = 1.09$ to ±3.2% at $(B/A)_{0.1} = 2.76$ in a manner similar to the τ, τ/σ_G curve shown in Figure 2. [e] Error limits reported for $t_G/\sigma_G = 20$. For $t_G/\sigma_G > 20$, the error limits will be smaller than those reported.

Table VI. Precision[a] Comparison of Three Graphical Methods for Estimating N_{SYS}, M_2, and σ_G

CFOM/ method	Gaussian eqs	empirical eqs, Table III, this work	calibration curve method reported previously (*18*)
N_{SYS}	±2.0	±2.5	±5
$\bar{M}_2$	±2.0	±2.4	±3
σ_G	±1.0	±2.0	±3

[a] Reported as percent relative standard deviation (%RSD). Precision of equations estimated via error propagation, using data of Table VII.

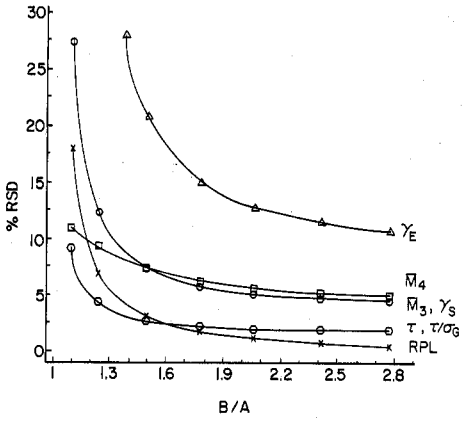

Figure 2. Dependence of precision on peak asymmetry for several CFOMs. The precision of all other CFOMs (N_{SYS}, $\bar{M}_2$, etc.) is essentially independent of peak shape and is included in Tables III–VI.

assuming the independence of the RSDs on peak shape.

The RSDs for t_R, W_α, and $(B/A - 1)_\alpha$ for individual peak shapes were originally reported relative to σ_G, σ_G, and $(B/A - 1)_\alpha$, respectively. Multiplication by σ_G/t_R, σ_G/W_α, and $(B/A - 1)_\alpha/(B/A)_\alpha$ converted them to the appropriate form.

Since the RSDs of t_R, W_α, and $(B/A)_\alpha$ were assumed to be independent of peak shape, intuitively it might seem that this should also be true for the RSD of any calculated CFOM. This is not the case, however. For one group of CFOMs (N_{SYS}, $\bar{M}_2$, σ_G, t_G, N_{MAX}, RSE, and M_1), a slight to moderate variation in RSD with $(B/A)_\alpha$ was observed. This can be explained by

Table VII. Suggested Chromatographic Measurement Conditions and the Relative Standard Deviations of t_R, W_α, and $(B/A)_\alpha$ Achieved

Conditions

1. Chromatogram recording rate: 1 cm/σ_G ($W_{0.1} \geq 4.3$ cm)
2. Ruler resolution: ±0.2 mm
3. Minimum retention distance, $(t_R)_{MIN}$: 10 cm
4. Minimum peak height, $(h_p)_{MIN}$: 10 cm

Results[a,b]

CFOM	%RSD (α = 0.1)	%RSD (α = 0.3)	%RSD (α = 0.5)
t_R	±0.2	identical	identical
W_α	±1.0	±1.0	±1.0
$(B/A)_\alpha$	±2.0	±2.5	± 3.0

[a] Data obtained from ref 19 and subsequently converted (see Detailed Discussion of Precision) for α = 0.1, 0.5—results interpolated for α = 0.3. [b] %RSD (t_R) rounded to nearest 0.1%; %RSDs for W_α, $(B/A)_\alpha$ rounded to nearest 0.25%.

examining the random error propagation in the general empirical equation

$$N_{SYS} = \frac{C_1(t_R/W_\alpha)^2}{(B/A)_\alpha + C_2}$$

Assuming negligible covariances, RSD(N_{SYS}) is given by

$$\mathrm{RSD}\,(N_{SYS}) = \Bigg[\underbrace{4\left(\frac{\sigma_{t_R}}{t_R}\right)^2}_{1} + \underbrace{4\left(\frac{\sigma_{W_\alpha}}{W_\alpha}\right)^2}_{2} + \underbrace{\left(\frac{\sigma_{(B/A)_\alpha}}{(B/A)_\alpha}\right)^2}_{3}\underbrace{\left(\frac{(B/A)_\alpha}{(B/A)_\alpha + C_2}\right)^2}_{4}\Bigg]^{1/2} \quad (12)$$

Even when terms 1–3 in eq 12 are constant, RSD(N_{SYS}) will vary somewhat with $(B/A)_\alpha$ because of term 4. Clearly this variation will be greatest for $-(B/A)_\alpha \leq C_2 \leq 0$. Additionally, as $C_2 \rightarrow -(B/A)_\alpha$, RSD($N_{SYS}$) $\rightarrow \infty$. For $C_2 \approx 0$, RSD(N_{SYS}) is essentially independent of $(B/A)_\alpha$. Finally, for $C_2 > 0$, a negligible to slight variation of RSD(N_{SYS}) with $(B/A)_\alpha$ may be observed, depending on the magnitude of terms 1 and 2 relative to the product of terms 3 and 4. Except for the first

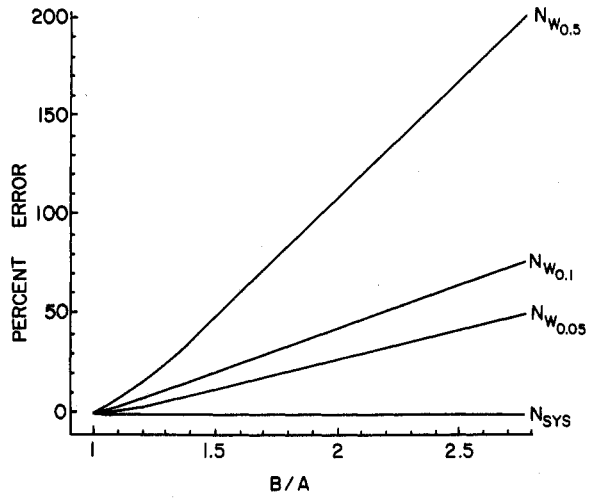

Figure 3. Relative error in plate count of three Gaussian equations (based on the indicated peak width measurements) and the EMG-based N_{SYS} equation (Table III, eq 1) for ideal and skewed peaks.

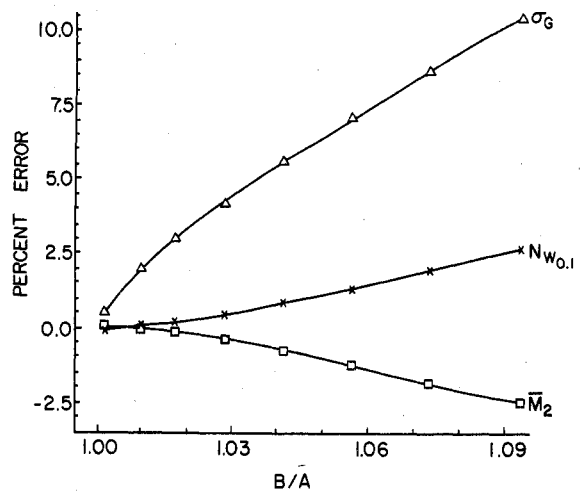

Figure 4. Relative error in the Gaussian standard deviation, plate count, and second central moment for Gaussian equations based on t_R, $W_{0.1}$ measurements for ideal and slightly skewed peaks.

three equations in Table V, the RSDs of N_{SYS}, $\bar{M}_2$, σ_G, t_G, N_{MAX}, RSE, and M_1 calculated via equations in Tables III, IV, and V varied by less than 0.5% for $1.00 \leq B/A \leq 2.76$.

The remaining CFOMs (τ, τ/σ_G, RPL, $\bar{M}_3$, γ_S, γ_E) comprise a second group whose RSDs are moderate to strong functions of peak shape as Figure 2 shows. In every instance the imprecision is largest for the least asymmetric peaks and smallest for the most highly skewed peaks. Analysis of the error propagation equations shows that one or more terms within the equations gets very large as the peak shapes become symmetric (*22*).

Why Measure at 10%? For reasons listed below, the recommended CFOM equations in Table III are based on (in addition to t_R) the measurement of W and B/A at 10% peak height rather than at other peak height fractions such as 50%, 30%, or 5%:

1. Examination of Tables III, IV, and V shows that many CFOM equations at 10% are clearly superior to the corresponding ones at 30% and 50% in terms of:
   (a) precision (lowest RSD limits)
   (b) widest working range for equivalent accuracy
   (c) simplicity for M_2 (path a)
2. The N_{SYS} equation at 10% peak height is more accurate for Gaussian and near-Gaussian peaks than other N_{SYS} equations developed at 50%, 30%, or 5% (*22*).
3. In a previously reported graphical measurement study (*19*), statistically significant positive and negative biases were detected in the measurement of $A_{0.5}$ and $B_{0.5}$, respectively, resulting in a consistent underestimation of $(B/A)_{0.5}$. No such biases were detected for $A_{0.1}$ and $B_{0.1}$, and only a slight underestimation was observed for $(B/A)_{0.1}$.
4. It is likely that $RSD(W_{0.05}) > RSD(W_{0.1})$, since in going from $W_{0.1}$ to $W_{0.05}$ the magnitude of the slope of the peak (on either side) decreases much more rapidly than the peak width increases. Thus the precision for the 5% CFOM equation would be poorer [assuming $RSD(W_{0.05})$ contributes substantially to the total uncertainty].
5. Superior resolution between overlapping peaks is required for measurements at 5% peak height than at 10%.
6. As exemplified in Figure 3 for N_{SYS}, Gaussian CFOM equations based on width measurements at 10% are much less inaccurate (though still exceedingly in error) for asymmetric peaks than the corresponding Gaussian equations at 50% (shown) and 30% (not shown). That is, the slope of the RE vs. $(B/A)_\alpha$ (shown for $\alpha = 0.1$) plots is smaller; thus the approximate RE correction function in the denominator of eq 2 and 5 (text) will be less sensitive to the measurement imprecision of $(B/A)_\alpha$.
7. The sensitivity of the RE correction functions to the $(B/A)_\alpha$ measurement imprecision is only slightly lower at 5% than at 10% peak height (see Figure 3) and is insufficient to warrant CFOM estimation at 5%.
8. The RSE can be calculated much more accurately by using an equation of the form of eq 8, Table III at 10% than at 50%, 30%, or 5%. In addition, the RSD limits are much lower at 10% than at 50% or 30% and are comparable to those at 5% (*22*).
9. The empirical asymmetry factor measurement, B/A, was introduced at 10% peak height rather than at 50% or 30% because peak tailing is much more apparent at 10%. Since then almost all empirical measurements of asymmetry have been reported at this peak height fraction; these data will be of little value in later years if the B/A peak height fraction is redefined.
10. It is easier to mentally compute 10% of an arbitrary peak height than 50%, 30%, or 5%.

Taken collectively, the above arguments indicate that *the best CFOM estimation is obtained from graphical chromatographic measurements at 10% peak height.*

What Type of Peak Shape? Chromatographic peaks should be examined for their resemblance to Gaussian, EMG, or other peak shapes, first by visual inspection and then from the asymmetry factor measurement. In the unlikely event that $B/A \approx 1$, the validity of the Gaussian model can be checked by comparing the measured peak width ratios $W_{0.5}$:$W_{0.3}$:$W_{0.1}$ to the theoretically predicted ratios 0.5487:0.7231:1. For $B/A \geq 1.09$, the validity of the EMG model can be judged by the agreement of values of σ_G, $\bar{M}_2$, and/or τ and t_G determined from both B/A and W measurements at $\alpha = 0.1$, 0.3, and 0.5 (see Tables III, IV, and V).

For slightly asymmetric chromatographic peaks, the assignment of peak shape models may be ambiguous due to the imprecise measurement of B/A (e.g., is a peak with $B/A = 1.03 \pm 0.02$ Gaussian?). Insofar as accuracy and precision are concerned, does it matter if EMG-based equations are used with Gaussian peaks or vice versa? As seen from Table III, the EMG base equations for N_{SYS}, $\bar{M}_2$, and σ_G are accurate to within ±1.5%, ±1.5%, and ±4%, respectively, over the asymmetry range $1.00 \leq B/A \leq 1.09$. Figure 4 shows the accuracy of the Gaussian based equations ($\alpha = 0.1$) over this same range. Clearly, little error in the estimation of $\bar{M}_2$, N_{SYS}, and σ_G will result from peak model misassignments at low asymmetries ($1.00 \leq B/A \leq 1.09$) due to B/A imprecision, though for $B/A \geq 1.04$ the EMG equations are more accurate. Furthermore, as seen from Table VI, the change in the precision of CFOM estimation resulting from peak model mis-

assignment would be less than 1%.

General Aspects of the Method. The universality of the relative error approach (introduced in the Derivations section above) was checked by the independent variation of t_G and σ_G over the t_G/σ_G range of 10 to 5000. The generality was confirmed by identical statistical results (%RELs, etc.) over a given B/A range (e.g., 1.09–2.76) for all CFOMs calculated from this approach.

As an additional check on the experimental work, $\bar{M}_2$ and N_{SYS} were calculated by statistical moment analysis (*10*), using the same t_R search algorithm as before (see Procedure). The agreement among the true, moment, and manual values for both $\bar{M}_2$ and N_{SYS} was within ±1% for $1.00 \leq B/A < 2.05$ with very little bias present in either approximation. At higher asymmetries ($2.05 \leq B/A \leq 2.76$), the manual values remained with ±1.5% of the true values, but the corresponding moment values showed a significant positive bias ranging from +1.5% to +5.5%. An even greater bias of +4.4% at $B/A = 2.05$ ($\tau/\sigma_G = 2$) reported elsewhere (*10*) was attributed to arbitrary data truncation. This was probably the source of bias in our statistical moment method as well, but regardless of the source of bias, the same conclusion may be drawn: at high asymmetries ($2.05 \leq B/A \leq 2.76$) the manual CFOM equation method is more accurate than the moment method.

Working Range of the Equations. The EMG-based equations were expected to be accurate over the asymmetry range used for the least squares curve fitting of the $f(B/A)$ approximations. Thus, except for eq 8, the accurate working range was thought to be $1.09 < B/A < 2.76$. Nevertheless, eq 1, 2(a,b), 6, 7, and 10 allow accurate estimation of N_{SYS}, $\bar{M}_2$, t_G, N_{MAX}, and M_1, respectively, for Gaussian shaped peaks ($B/A = 1.00$). Although somewhat surprising, this is explained by the near convergence of these EMG equations to Gaussian ones when the substitution $B/A = 1.00$ is made in the former. The N_{SYS} equation in Table III, for example, becomes

$$N_{SYS} = 18.53(t_R/W_{0.1})^2 \quad (13)$$

which is within +0.6% of the Gaussian formula

$$N_{W_{0.1}} = 18.42(t_R/W_{0.1})^2 \quad (14)$$

CFOM equations could have been developed for asymmetries greater than $B/A = 2.76$ ($\tau/\sigma_G = 3$), but a sacrifice of simplicity, accuracy, or both would have been required. More importantly, however, it was felt that nearly all peaks reported in the literature exhibit B/A's ≤ 2.76. Indeed, a chromatographic system producing peaks with B/A's > 2.76 is operating at a relative system efficiency of less than 10%.

When the EMG N_{SYS} equation was tested for asymmetries higher than those for which it was developed, the %RE varied between −1.5% and −10% for $2.77 \leq B/A \leq 4.00$, compared to the %RE range of +70% to +110% for the Gaussian 10% equation ($N_{W_{0.1}}$).

Real vs. Ideal CFOMs; Column Characterization. Given that peak asymmetry is (almost) always present in any real chromatographic system, N_{SYS}, $\bar{M}_2$, and t_R represent the experimentally observed chromatographic efficiency, peak variance, and retention time, respectively. The corresponding CFOMs N_{MAX}, σ_G^2, and t_G represent idealized chromatographic parameters which would describe the system if all sources of asymmetry could be eliminated. If all or nearly all asymmetry is extracolumn in origin, then for a given set of conditions N_{MAX}, σ_G^2, and t_G are valid descriptors of the efficiency, band-broadening, and retention characteristics of the *column*.

Pluralism of the Method. As might be surmised from Table III, there is more than one way to calculate several of the CFOMs. The variance, for example, can be calculated via eq 2a from measurements of $W_{0.1}$ and B/A or via eq 2b from t_R and N_{SYS} (eq 1). Generally, CFOM estimates via the "b" equations are simpler, faster, equally precise, but less accurate than estimates via the "a" equations. This trade-off of accuracy for simplicity and speed is slight, however; in most cases much time can be saved with little sacrifice in accuracy if the "b" equations are employed.

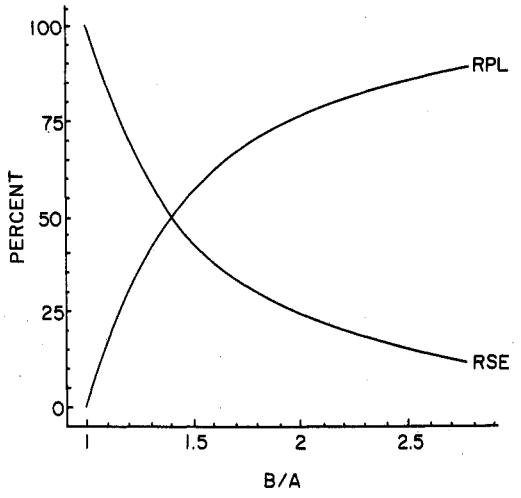

Figure 5. Relative system efficiency, RSE, and relative plate loss, RPL, for ideal and skewed peaks.

Only the simplest and most accurate methods are given in Table III. Therefore, while N_{SYS} could be calculated from its components t_R, σ_G, and τ (see N_{SYS} equation in Table II), this method was not reported since it would be much more time-consuming, tedious, and in all likelihood less accurate and less precise than the "wholistic" N_{SYS} equation in Table III.

Usefulness of RSE, RPL. The relative system efficiency (RSE) and relative plate loss (RPL), two new parameters defined in Table II, are dualistic CFOMs. First, they can be interpreted intuitively as N_{SYS}/N_{MAX} and $(N_{MAX} - N_{SYS})/N_{MAX}$, respectively, with a corrective retention factor $(t_G/t_R)^2$ applied. Alternatively, RSE and RPL can be viewed as the relative contributions of symmetrical (σ_G^2) and asymmetrical (τ^2) band-broadening processes to the total system band-broadening ($\bar{M}_2$, the total variance). If $(t_G/t_R)^2$ can be neglected because of its nearness to unity, the former intuitive expressions for RSE and RPL become particularly useful. For example, the best possible efficiency, N_{MAX}, can be related very simply to the true chromatographic efficiency, N_{SYS}, by

$$N_{MAX} = N_{SYS}/\text{RSE} \quad (15)$$

In fact, this approximation is good to within +2% with an RSD limit of ±5% (for $1.00 \leq B/A \leq 2.76$) whenever N_{MAX} (calculated via eq 15) > 4000. Thus, eq 15 can serve as a useful estimation of N_{MAX} for moderate to high efficiency chromatographic systems.

Although B/A, RSE, and RPL are mutually interdependent (i.e., once B/A has been measured RSE and RPL may be calculated), *the specification of RSE, RPL, or both* in addition to the reporting of *B/A greatly enhances the qualitative description of a chromatographic system.* Thus, while $B/A = 1.30$ indicates that a given peak is asymmetric, the corresponding RSE = 55% or RPL = 45% provides a clearer indication of the actual efficiency and how much room for improvement exists.

Figure 5 shows the exponential-like relationship of RSE and RPL with B/A. Chromatographic systems with asymmetries of 1.00 and 1.10 are operating at much different relative efficiencies, while two systems operating at $B/A = 2.00$ and 2.10 are realizing nearly the same relative efficiencies.

Alternative Derivations. Two other approaches for deriving CFOM equations were not as successful as that already

described. In the first attempt, a modification of the Carr graphical method, three universal calibration curves were approximated by linear or quadratic polynomials. This approach yielded equations for σ_G, τ, t_G, and the remaining CFOMs in terms of $W_{0.1}$, B/A, and t_R, but is unsatisfactory for three reasons: (a) an accurate but simple approximation of τ/σ_G in terms of B/A cannot be obtained for the range $1.00 \leq B/A \leq 2.76$ because the relationship between them changes at $B/A = 1.36$ from a decidedly nonlinear one to an almost perfectly linear one; (b) the errors introduced by the polynomial approximations tend to accumulate slightly rather than cancel; and (c) the equations derived for all the CFOMs except, τ, σ_G, and t_G are extremely unwieldly, e.g.

$$N_{SYS} = (t_R/W_{0.1})^2[g(B/A)/h(B/A)] \qquad (16)$$

where g and h are second degree polynomials of B/A. A variation of this same approach in which B/A was substituted for the original abscissa τ/σ_G in the latter two calibration curves made little difference.

Another try, a variation of the relative error approach utilizing $(B - A)$ as the approximation G in eq 5 for τ, failed because the simplest $f(B/A)$ approximation required for sufficient accuracy was too complex.

CFOM Units. For ease of interlaboratory comparison, all nonunitless CFOMs should be reported in time units; if units of length are chosen instead, the recorder chart speed should be specified to permit conversion to time units.

Superiority of EMG-Based Equations. Although Gaussian-based equations are somewhat simpler than their EMG counterparts in Table III (compare eq 14, text, with eq 1, Table III), the EMG equations are to be much preferred. They exhibit comparable precision (see Table VI) and are equally accurate for Gaussian (or near-Gaussian) peaks and considerably more accurate for skewed (EMG) chromatographic peaks. Adoption of the equations in Table III, especially

$$N_{SYS} = \frac{41.7(t_R/W_{0.1})^2}{B/A + 1.25}$$

is strongly urged.

LITERATURE CITED

(1) Snyder, L. R.; Kirkland, J. J. "Introduction to Modern Liquid Chromatography", 2nd ed.; Wiley: New York, 1979.
(2) Giddings, J. C. *Anal. Chem.* **1963**, *35*, 1999–2002.
(3) Kucera, E. *J. Chromatogr.* **1965**, *19*, 237.
(4) Karger, B. L.; LePage, J. N.; Tanaka, N. "High Performance Liquid Chromatography, Advances and Perspectives"; Horvath, C., Ed.; Academic Press: New York, 1980; Vol. 1, pp 119–121.
(5) Schmuach, L. J. *Anal. Chem.* **1959**, *31*, 225–230.
(6) Johnson, H. W., Jr.; Stross, F. H. *Anal. Chem.* **1959**, *31*, 357–365.
(7) Sternberg, J. C. "Advances in Chromatography"; Giddings, J. C., Keller, R. A., Eds.; New York: Marcel Dekker: 1966; Vol. 2, pp 205–270.
(8) McWilliam, I. G.; Bolton, H. C. *Anal. Chem.* **1969**, *41*, 1755–1770.
(9) Pauls, R. E.; Rogers, L. B. *Sep. Sci.* **1977**, *12*, 395–413.
(10) Kirkland, J. J.; Yau, W. W.; Stoklosa, H. J.; Dilks, C. H. *J. Chromatogr. Sci.* **1977**, *15*, 303–316.
(11) Pauls, R. E.; Rogers, L. B. *Anal. Chem.* **1977**, *49*, 625–628.
(12) Haddad, P. R.; Keating, R. W.; Low, K. C. *J. Liq. Chromatogr.* **1982**, *5*, 853–867.
(13) Maynard, V.; Grushka, E. *Anal. Chem.* **1972**, *44*, 1427–1434.
(14) Grushka, E.; Myers, N. M.; Schettler, P. D.; Giddings, J. C. *Anal. Chem.* **1969**, *41*, 889–892.
(15) Chesler, S. N.; Cram. S. P. *Anal. Chem.* **1971**, *43*, 1922–1933.
(16) Yau, W. W. *Anal. Chem.* **1977**, *49*, 395–398.
(17) Grushka, E. *Anal. Chem.* **1972**, *44*, 1733–1738.
(18) Barber, W. E.; Carr, P. W. *Anal. Chem.* **1981**, *53*, 1939–1942.
(19) Carr, P. W., University of Minnesota, Minneapolis, Minnesota, personal communication, supplementary material from ref 18.
(20) Abramowitz, M., Stegun, I. A., Eds. "Handbook of Mathematical Functions"; National Bureau of Standards: Washington, DC, 1964; Applied Mathematics Series No. 55, p 932.
(21) Bevington, P. F. "Data Reduction and Error Analysis for the Physical Sciences"; McGraw-Hill: New York, 1969; pp 56–64.
(22) Foley, Joe P.; Dorsey, John G., unpublished work, 1982.

RECEIVED for review August 13, 1982. Accepted December 22, 1982. This work was presented in part at the 184th National Meeting of the American Chemical Society, in Kansas City, MO, on Sept 5, 1982.